Fluorescence Energy-Transfer Probes of Conformation in Peptides: The 2-Aminobenzamide/Nitrotyrosine Pair

Jens Ø. Duus* and Morten Meldal

Carlsberg Laboratory, Department of Chemistry, Gamle Carlsberg Vej 10, DK-2500 Valby, Denmark

Jay R. Winkler*

Beckman Institute 139-74, California Institute of Technology, Pasadena, California 91125

Received: October 15, 1997; In Final Form: June 9, 1998

The photophysical properties of the fluorescence energy-transfer donor, 2-aminobenzamide (Abz), and nitrotyrosine (Tyr−NO_2) acceptor have been evaluated. The 31-Å Förster radius for this donor−acceptor pair makes it useful for evaluating molecular separations in the range of 15−45 Å. Abz and Tyr−NO_2 have been incorporated into four medium-sized synthetic peptides (**1**, Abz-SEEEEKKKKEEEEKKKK(Tyr(NO_2))D; **2**, Abz-AEAAAKHAAAHEAAAKA(Tyr(NO_2))D; **3**, Abz-FAQKEPAFLKEYHLL(Tyr(NO_2))D; **4**, Abz-LKELKDKLKELKDKLK(Tyr(NO_2))LKD). Nonexponential Abz fluorescence decays indicate that the synthetic peptides do not assume single, static conformations in solution. The fluorescence decay kinetics in three of the four peptides have been fit to a model in which the peptide conformations are described by Gaussian distributions of donor−acceptor distances centered at r_C (r_C (fwhm): **2**, 27.0 (8.1); **3**, 25.6 (12.9); **4**, 21.1 (22.1) Å). Values of r_C are in good agreement with distances obtained from molecular dynamics simulations (r_{MD}: **2**, 28; **3**, 21; **4**, 22 Å).

Introduction

The conformations of peptides and proteins play a pivotal role in defining their functions. The unique three-dimensional fold of a protein represents the global free energy minimum in the vast conformational space of the constituent polypeptide. Complex formation or substrate binding can induce a conformational change that modulates the activity of a protein. Structural changes of this type provide a means of regulation and control in biochemical transformations. On a smaller scale are medium-sized peptides (10−20 amino acids), which perform important signaling and regulatory functions and are finding increasing application in the development of modern drugs. In contrast to globular proteins, the energy differences among different conformations of medium-sized peptides are small ($<k_BT$) and the barriers to interconversion are relatively low. Consequently, medium-sized peptides are dynamic molecules that rapidly interconvert among several distinct conformations. Complete characterization of the physical, chemical, and dynamical properties of these peptides is essential for a thorough understanding of their interactions with receptors. In particular, the conformations of small peptides, as well as the dynamics of interconversion among conformations, can play a critical role in defining interactions with larger biomolecules.

There are several spectroscopic probes of protein and peptide conformation that provide complementary structural information spanning a wide range of time scales. Circular dichroism (CD) spectroscopy, for example, reports on the aggregate secondary-structure content of a sample. Although the radiation−molecule interaction time in CD spectroscopy is very short ($<10^{-13}$ s), time-resolved measurements face significant technical challenges.[1] Nuclear magnetic resonance (NMR) spectroscopy can provide residue-specific information about the average conformations of proteins and peptides in solution,[2] but dynamical information is limited to relatively slow (10^{-5}−10^{-3} s) time scales.

Time-resolved fluorescence energy-transfer measurements provide a unique piece of structural information. The kinetics of energy transfer depend directly upon the distribution of distances between a fluorophore and acceptor. Energy-transfer partners incorporated into a single molecule or two interacting molecules will furnish site-specific conformational detail. Förster's model of fluorescence energy transfer is generally used to extract donor−acceptor distances from fluorescence decay kinetics.[3] Depending on the chromophores being used, donor−acceptor separations as large as 100 Å can be evaluated.[4] Furthermore, resonance energy-transfer measurements can provide dynamical information in the time regime from 10^{-11} to 10^{-8} s.[4−6] These methods are finding wide application in studies of protein-folding dynamics and peptide conformational dynamics and in screening combinatorial libraries.[7−10]

To obtain useful distance information from resonance energy-transfer measurements, the photophysical properties of the donor−acceptor pair must be thoroughly characterized. A particularly important parameter is the Förster distance (R_0), the donor−acceptor separation at which the energy-transfer rate equals the luminescence decay rate of the isolated donor. In studies of proteins and peptides, it is particularly important that the probes do not significantly perturb the conformational energetics or dynamics of the host molecule. Many energy-transfer probes are large aromatic (hence, hydrophobic) groups that are not likely to meet this criterion. An exception is the 2-aminobenzamide−nitrotyrosine (Abz−Tyr(NO_2)) pair in which both chromophores are small polar amino acid side chains. These probes have been employed previously as internally quenched fluorescent substrates for endopeptidases[11] and are

S1089-5647(97)03352-X CCC: $15.00
Published on Web 07/29/1998

readily incorporated in solid-phase peptide synthesis. This pair has also proven to be useful in screening combinatorial peptide libraries[8] and for studies of peptide−peptide[10] and peptide−protein interactions.[9] In proteins, the Abz donor can be introduced selectively to surface sites, and Tyr residues can be nitrated under relatively mild conditions, to provide site-specific probes of folding.[7,12] The photophysical properties of this energy-transfer pair, however, have not been thoroughly explored. In particular the R_0, which determines the range of distances that can be explored, has not yet been determined. The present work is an examination of the Abz−Tyr(NO_2) donor−acceptor pair for its suitability as a long-range energy-transfer probe in studies of protein and peptide conformations and dynamics.

Background

The rate constant for fluorescence energy transfer (k_{et}) depends, to a first approximation, on the excited-state lifetime of the unquenched fluorophore (τ_D), an effective interaction radius known as the Förster distance (R_0), and the donor−acceptor distance (r, eq 1).[3,4]

$$k_{et} = \frac{1}{\tau_D}\left(\frac{R_0}{r}\right)^6 \tag{1}$$

The Förster distance depends on the physical and spectroscopic properties of the chromophores and the surrounding medium (eq 2).[4,5]

$$R_0^{\,6} = 8.785 \times 10^{-5}\,\frac{\kappa^2 \Phi_D J}{n^4} \tag{2a}$$

$$J = \int F_D(\lambda)\,\epsilon_A(\lambda)\lambda^4\,\mathrm{d}\lambda \tag{2b}$$

The orientation factor (κ) assumes an average value of $^2/_3$ for random uncorrelated orientation of the donor and acceptor (vide infra), ϕ_D is the donor fluorescence quantum yield, n is the refractive index of the solution, and the integral J describes the overlap between the normalized donor fluorescence spectrum (F_D), the acceptor molar absorption spectrum (ϵ_A), and the fourth power of the wavelength (λ). R_0 determines the useful distance range for an energy-transfer donor−acceptor pair. The response speed of the fluorescence lifetime apparatus defines the short-range limit; the long-range limit depends on the precision with which fluorescence decay rates can be determined.

Experimental Section

Materials. The four peptides used in this study (**1**−**4**) were prepared using multicolumn peptide synthesis (MCPS):[11,13,14]

1: Abz-SEEEEKKKKEEEEKKKK(Tyr(NO_2))D
2: Abz-AEAAAKHAAAHEAAAKA(Tyr(NO_2))D
3: Abz-FAQKEPAFLKEYHLL(Tyr(NO_2))D
4: Abz-LKELKDKLKELKDKLK(Tyr(NO_2))LKD

2-Aminobenzoic acid, 3-nitro-L-tyrosine, and quinine bisulfate were purchased from Fluka and used without further purification. The peptide chromophore precursors, 2-*tert*-butyloxycarbonylamino benzoate, 3,4-dihydro-4-oxo-1,2,3-benzotriazol-3-yl 2-*tert*-butyloxycarbonylamino benzoate, and N^{α}-fluoren-9-ylmethyloxycarbonyl-3-nitrotyrosine were prepared as described previously.[11]

MCPS[13,14] *of Fluorescence-Quenched Model Compounds* ***1***−***4***. Resin (50 mg, 0.19 mmol/g) derivatized with hydroxymethylbenzamide and esterified with Fmoc-Asp(*t*Bu)-OH using the 2,4,6-mesitylenesulfonyl-3-nitro-1,2,4-triazolidine procedure[15] was packed into each column of a 96 column Teflon synthesis block containing a PTFE filters at the bottom.[13,14] The quenched peptides were synthesized simultaneously in four columns with other unrelated syntheses in the residual 92 columns. The resin in the 96 columns was deprotected with 20% piperidine in DMF (2 × 40 mL, 1 and 10 min) and washed successively with DMF (5 × 45 mL). For the four columns Fmoc-Tyr(NO_2)-OH (51 mg, 0.11 mmol) was activated 15 min at room temperature with *O*-(1*H*-benzotriazol-1-yl)-*N*,*N*,*N*′,*N*′-tetramethyluronium tetrafluoroborate (22 mg, 0.11 mmol) and *N*-ethylmorpholine (14 μL, 0.11 mmol) in DMF (2 mL), and the solution was added to the resin. After 15 h the reagents were removed by suction, and the 96 columns were washed with DMF (5 × 45 mL), treated with 20% piperidine in DMF (2 × 40 mL, 2 and 15 min), and washed with DMF (5 × 45 mL). Fmoc-amino acid-OPfp (8 mg, 3 equivalents/column) and Dhbt-OH (3 mg, 3 equiv/column) were dissolved in DMF (400 μL/column) and added to the resin. The reaction was left for a period of 2 h (or 24 h for difficult couplings) with agitation, and the reagents were removed by suction. Deprotection and washing was as described above. After assembly of the entire peptide sequence, Boc-ABz-ODhbt (50 mg, 3 equiv/column) was dissolved in DMF (2 mL) and added to the four columns. The reaction was left for a period of 16 h with agitation, and the reagents were removed by suction. The cycle of washing, deprotection, and coupling was repeated as described above. The columns were washed with dichloromethane (5 × 45 mL) and dried under high vacuum. The resin was treated for 2 h with 95% aqueous trifluoroacetic acid (TFA), the TFA was removed by suction, and the resin was washed with dichloromethane (6 × 45 mL) and DMF (3 × 45 mL) and neutralized with 2% piperidine in DMF (2 × 40 mL). After final washings with DMF (5 × 45 mL) and dichloromethane (5 × 45 mL), the substituted resin was dried in vacuo. Peptides **1**−**4** were cleaved off the resin with 0.1 M NaOH solution 350 μL/column for 2 h, and the products were eluted from the column and neutralized with 0.1 M HCl. The peptides obtained in 40−55% crude yield were dissolved in a small amount of DMF and purified by HPLC using buffer A (0.1% aqueous TFA) and B (10% A in CH_3CN) with a gradient of 0%−100% B in 1 h on a semipreparative radical pack RP-C_{18} column and a Waters HPLC system with 80 mL/min pump heads and a diode array detector. The pure peptides were isolated in yields of 10−20%, and their compositions were confirmed by sequence analysis on an ABI 430 gas-phase sequencer.

Methods. All steady-state and time-resolved spectra were recorded at room temperature with samples dissolved in tris(hydroxymethyl)aminoethane (TRIS) buffer (50 mM, pH 8.5). Samples were deoxygenated by repeated evacuation/Ar-fill cycles and sealed in fused-silica fluorescence cuvettes (1 cm × 1 cm).

Steady-State Spectroscopy. Absorption spectra for quantum-yield studies were measured using a refurbished Cary 14 spectrophotometer (OLIS). Routine absorption spectra were measured using a Hewlett-Packard 8452A diode array spectrophotometer. Fluorescence spectra were recorded with a custom-built instrument (Caltech).[16] Samples were excited with the 312.6-nm emission line from a Hg−Xe arc lamp. Spectra were collected with 2-nm resolution between 350 and 600 nm.

Absolute luminescence quantum yields were determined by the method of Demas and Crosby for optically dilute samples.[17] The quantum-yield standard was quinine bisulfate in 1.0 N

sulfuric acid, which has an absolute fluorescence quantum yield of 0.55.[18] The excitation wavelength was the same for both samples (312.6 nm), and the refractive indices for the two solutions were taken to be identical. Reported quantum yields represent averages of several different measurements at different sample concentrations (all with absorbances below 0.1 at 312.6 nm).

Evaluation of the Förster Distance. The value of J (eq 2b) for the Abz−Tyr(NO_2) donor−acceptor pair was determined on the basis of several measurements of both Abz−Gly fluorescence and Tyr(NO_2) absorption, at concentrations between 20 and 100 μM. The solution refractive index was taken to be 1.34.[19]

Time-Resolved Spectroscopy. Fluorescence decay measurements were performed using the method of time-correlated single-photon counting (TCSPC).[20] The excitation source was a cavity-dumped dye laser synchronously pumped by a frequency-doubled (532 nm) mode-locked Nd:YAG laser (Coherent Antares). The dye was 4-dicyanomethylene-2-methyl-6-(*p*-dimethylaminestyryl)-4*H*-pyran (DCM, Kodak) in ethylene glycol/benzyl alcohol operating at a fundamental wavelength of 640 nm. Dye-laser output was frequency-doubled (320 nm) using a β-barium borate (BBO) crystal. The pulse repetition rate was set to 3.8 MHz.

Sample fluorescence was collected at a 90° angle to an excitation beam polarized perpendicular to the plane formed by excitation and collection paths. A polarizer was oriented to collect light polarized at the "magic angle" for measuring excited-state decay kinetics, or parallel or perpendicular to the excitation polarization direction for time-resolved fluorescence anisotropy measurements.[20] After passing through the analyzing polarizer, sample fluorescence was wavelength-selected with a monochromator (McPherson 270, 0.35 m, f/4) and detected using a microchannel plate photomultiplier (Hamamatsu R2949HA) cooled to −40 °C. Single-photon pulses from the photomultiplier were amplified (Hewlett-Packard 8447F) and sent to a constant fraction discriminator (CFD, Ortec 934). The experiments were performed with the photomultiplier pulses generating start signals (reverse timing mode). Stop pulses, generated by directing some residual 640-nm dye-laser output onto a silicon photodiode (Thorlabs), were delayed (Ortec 425A) and then sent to the CFD. Start and stop pulses were fed into a time to amplitude converter (Tennelec TC 864), the output of which was directed to a multichannel analyzer (4096 channels, Ortec Spectrum Ace). Fluorescence decay signals were acquired with 5−20 μM peptide solutions until 10^4 counts had accumulated in the channel at the peak of the decay curve.

Fluorescence anisotropy measurements were performed by collecting decay curves with parallel ($I_{||}(t)$) and perpendicular ($I_{\perp}(t)$) orientations of a polarizer before the entrance slit of the monochromator. The time-dependent anisotropy ($r(t)$) was evaluated using eq 3 after scaling $I_{||}(t)$ and $I_{\perp}(t)$ on the long-time tails.[20]

$$r(t) = \frac{I_{||}(t) - I_{\perp}(t)}{I_{||}(t) - 2I_{\perp}(t)} \tag{3}$$

Data Analysis. Observed fluorescence decays ($I(t)$) are convolutions of the intrinsic fluorescence decay function ($f(t)$) with the instrument response function ($R(t)$, eq 4).[21]

$$I(t) = \int_0^t R(t)\, f(t - x)\, \mathrm{d}x \tag{4}$$

Instrument response functions for the TCSPC apparatus were extracted from the derivatives of the fluorescence decay profiles of a dye known to exhibit clean single-exponential excited-state decay kinetics (2-(4-biphenyl)-6-phenylbenzoxazole (PBBO) in dioxane, $\lambda_{OBSD} = 420$ nm,[22] $\tau_{OBSD} = 1.1$ ns).[21] The amplitudes of reconvolved decay profiles using this response function match those of the experimental functions to within 1% (fitting gave reduced chi-squared values of $\chi_R^2 = 1.2$). Fluorescence decay kinetics were fit by iterative reconvolution using the response function determined with PBBO. The full width at half-maximum of this instrument response function is on the order of 50 ps.

Fluorescence decay kinetics were fit to three different intrinsic decay functions: single-exponential, biexponential, and continuous distributions of single-exponential decays. In the latter case, we assumed a Gaussian distribution of donor−acceptor distances to define the distribution of first-order decay constants according eq 1.[5] All fitting was accomplished using MATLAB or custom-written software.

Molecular Modeling. Peptides were constructed in the Insight modeling package from Biosym (San Diego, CA), and molecular dynamics (MD) were performed on a SGI R8000-based workstation. The MD calculations were carried out in the CVFF force field with standard potentials and partial charges.[23] The MD calculations were performed without explicit inclusion of water molecules; a continuous medium of dielectric constant equal to 80 was used instead. MD simulations were performed for 300-ps intervals with time steps of 1 fs at 300 K after minimization and equilibration for 10 ps. Constrained MD calculations were performed by restricting the peptide backbones to α-helical conformations using a cosine potential for the dihedral angles of the backbone.

Donor−acceptor distances were measured from the mass midpoints of the phenyl groups in Abz and Tyr(NO_2). The relative orientations of the donor and acceptor were defined using vectors from the mass midpoints to the substituent nitrogen atoms of each ring.

Results and Discussion

The Peptides. The four peptides synthesized for this study are derived from sequences that have been investigated previously using other methods.[24−27] Deviations from the earlier sequences, such as the inclusion of the fluorescence donor/acceptor pair, are relatively minor.

Peptides **1**−**4** have varying degrees of α-helicity. Ions pairs between side chains at positions i and $(i + 4)$ were designed to stabilize the α-helical conformation in two previously studied close analogues of **1** and **2**; CD spectroscopy supports this structure.[24,25] An amphipathic α-helix in **3** was designed to be a synthetic T-cell antigen. The proline residue at position 6 is believed to disrupt partially the α-helical structure.[26] CD measurements indicate that an analogue of **4** is not highly helical and can be readily unfolded by guanidine hydrochloride.[27]

The Förster Distance. The first step in using fluorescence energy transfer to the measure molecular distances and dynamics is the evaluation of the Förster distance, R_0.[4,5] A fluorescence quantum yield of $\phi_D = 0.53$ was determined for Abz attached to a glycine residue, and the value of $J = 1.16 \times 10^{14}$ $M^{-1}cm^{-1}nm^4$ (eq 2b) was determined from the overlap of the Abz fluorescence and Tyr(NO_2) absorption spectra (Figure 1). For this donor−acceptor pair, then, we find that $R_0 = 31$ Å for randomly oriented donors and acceptors ($\kappa = {}^2/_3$). The fluorescence decay of the Abz−Gly model compound can be described by a single-exponential function with a decay constant

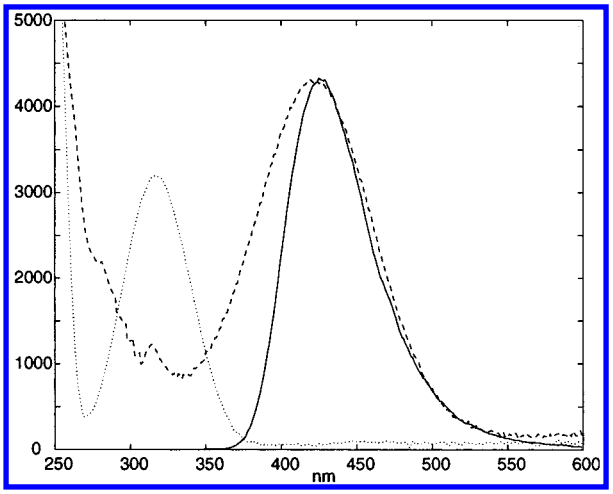

Figure 1. Fluorescence spectrum of Abz−Gly (solid line), and molar absorption spectra of Abz−Gly (dotted line) and Tyr(NO_2) (dashed line) (TRIS buffer, pH 8.5).

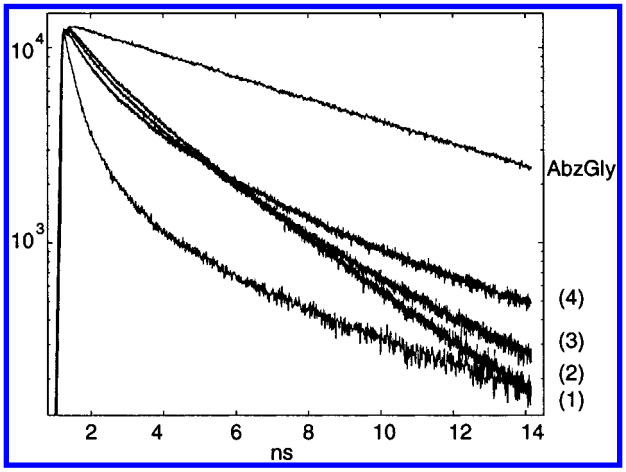

Figure 2. Plots of fluorescence decay kinetics of Abz−Gly and **1**−**4**.

of $\tau_D = 7.6$ ns ($\lambda_{OBSD} = 420$ nm, $\chi^2_R = 1.3$).[28] Hence, with our equipment, the 2-aminobenzamide−nitrotyrosine donor−acceptor pair is useful for measuring molecular separations in the range of 15−45 Å.

Fluorescence Quenching in Peptides. Incorporation of the Abz chromophore into four short peptides containing Tyr(NO_2) (**1**−**4**) significantly accelerates fluorescence decay and the kinetics no longer can be described by single-exponential functions (Figure 2). The Abz fluorescence decay time is shortened by about a factor of 4 in **2**−**4** and by about a factor of 15 in **1**. Substituting these approximate decay times into eq 1 and solving for *r* gives donor−acceptor distances in **2**-**4** of ∼26 Å, and ∼21 Å in **1**.

The nonexponential fluorescence decay in **1**−**4** indicates that the peptides do not assume a single static conformation in solution and that the different conformations interconvert on time scales slower than that of excited Abz (*Abz) decay. Similar results have been found with other fluorescence donor−acceptor pairs bound to peptides.[4,6] The slow conformational exchange (relative to *Abz decay) is consistent with laser-temperature-jump studies of helix melting and formation in a small (21-residue) alanine-based peptide.[29] If the peptides adopt two slowly exchanging conformations (with different values of *r*), then *Abz decay would be biphasic. Indeed, improved fits to the data are obtained using biexponential decay functions (Table 1), although the χ^2_R values are still quite large.

TABLE 1: Fitting Results for *Abz Fluorescence Decay in 1−4[a]**

sample	r_2 (α_1) Å	r_2 (α_2) Å	χ^2_R [b]	r_C, Å	fwhm, Å	χ^2_R [b]	r_{MD}, Å
1	19.4 (0.87)	34.6 (0.13)	7.94		*d*		27
2	25.0 (0.12)	30.8 (0.88)	7.01	27.0	8.1	1.49	28
3	20.4 (0.41)	28.9 (0.59)	7.30	25.6	12.9	1.14	21
4	19.7 (0.88)	29.7 (0.12)	9.80	21.1	22.1	1.61	22
PBBO				24.0	1.5	0.89[c]	

[a] Donor−acceptor distances (r_1, r_2) and weights (α_1, α_2) are from biexponential decay functions. Mean values (r_C) and full widths at half-maximum (fwhm) are from fits to Gaussian distributions of donor−acceptor distances. Donor−acceptor distances obtained from molecular dynamics simulations (r_{MD}) are shown for comparison. [b] Reduced chi-squared. [c] The value of χ^2_R probably reflects the uncertainty in our estimates of the errors in each intensity measurement. [d] Acceptable fits could not be obtained using a Gaussian distribution.

Rather than just two conformations, it is possible that the peptides can be described by a distribution of conformations and, hence, donor−acceptor distances. The data were, therefore, fit using static Gaussian distributions of donor−acceptor distances (*r*).[5] To test this fitting procedure, we have fit the single-exponential PBBO fluorescence decay to a Gaussian distribution assuming $\tau_D = 7.6$ ns (the value for Abz). A relatively narrow distribution (1.5 Å, full width at half-maximum (fwhm)) centered at a 24 Å provides the best fit. Substituting this value for *r* into eq 1 gives an excited-state lifetime of 1.1 ns, in good agreement with the value extracted from fits to an exponential decay function. The results of fitting fluorescence decay kinetics in **1**−**4** to the distributed model are summarized in Table 1. *Abz decay in **2** can be described by a single Gaussian distribution centered at $r_C = 27$ Å, with an 8-Å fwhm. A broader distribution (12.9-Å fwhm) centered at a somewhat shorter distance (25.6 Å) gives the best fit to the fluorescence decay kinetics in **3** (Figure 3). A bimodal distribution is required to fit the fluorescence decay of **4**. In this case, most of the fluorescence quenching can be attributed to a single distribution; the minor component is characterized by a broad distribution centered at large *r*. The *Abz quenching due to the minor component is quite small, and simulations indicate that this distribution is barely distinguishable from that of the unquenched model complex. It is possible, then, that this slow component of the excited-state decay kinetics is due to a minor (<5%) impurity in the sample. The *Abz decay in **1** could not be fit with single or bimodal Gaussian distributions in *r*. The substantially faster *Abz decay in **1** (compared to **2**−**4**) indicates a shorter Abz−Tyr(NO_2) distance, possibly because of a folded structure or the formation of dimers or aggregates. It is possible that unsymmetrical or rapidly exchanging distributions are required to fit these data. The widths of the distributions are a reflection of the flexibility of the peptides. The narrow 8.1-Å distribution for **2** is consistent with the high degree of helicity indicated by CD measurements,[25] while the broader 22.1-Å distribution of **4** is expected for a less helical, readily denatured peptide.[27] A helix disrupted by a proline turn or bend could produce the intermediate width of the distribution for **3** (12.9 Å).[26]

It is interesting to compare the results from the time-resolved energy-transfer studies to estimates of the donor−acceptor distances based on molecular dynamics simulations. Calculations performed without any restraints generally gave very compact structures, probably owing to the absence of solvent water molecules. To estimate donor−acceptor distances, calculations were performed on peptides with constrained backbone conformations. Chou−Fassman profiles indicate a high propensity for α-helical conformations in the four peptides that

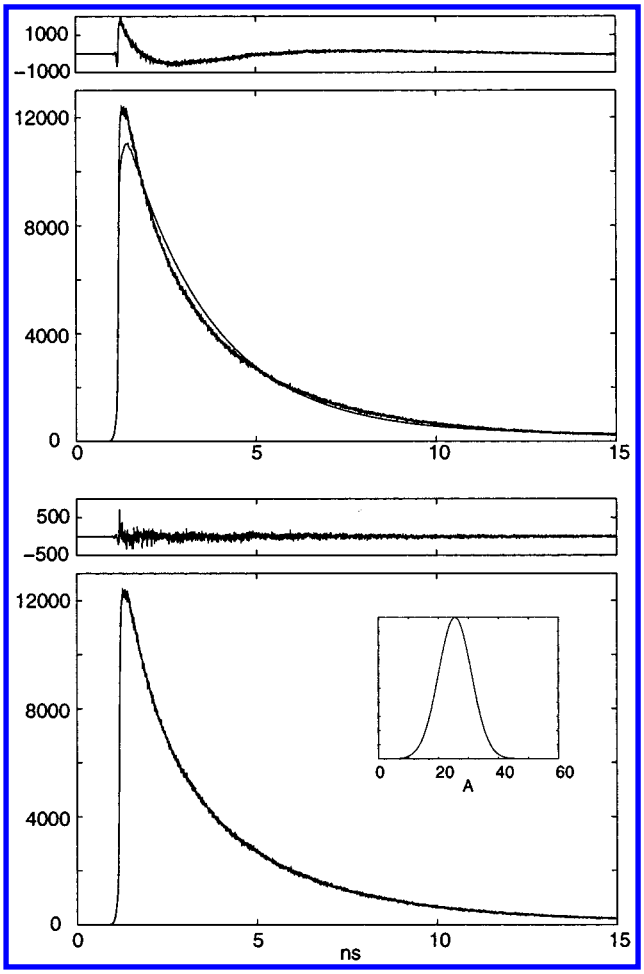

Figure 3. Fluorescence decay kinetics for **3**: (upper) best fit to a single-exponential decay function ($\chi^2_R = 16.3$); (lower) fit to a single Gaussian distribution in r centered at 25.6 Å with a full width at half-maximum of 12.9 Å ($\chi^2_R = 1.14$). The inset shows the best-fit distance distribution for **3**.

we have examined,[30] and CD measurements on close analogues indicate medium-to-high degrees of α-helicity.[24−27] We, therefore, performed molecular dynamics simulations in which the sequences of **1**−**4** were constrained to adopt α-helical backbone conformations, except for the residues around Pro in **3** where secondary-structure analysis indicated a turn. The average donor−acceptor distances extracted from these calculations are summarized in Table 1.

Fluorescence Anisotropy Measurements. Irradiation of Abz with a polarized laser pulse creates a spatially oriented population of *Abz molecules. Initially, the polarization of the fluorescence from *Abz will be anisotropic; as the orientation of *Abz molecules becomes random, the fluorescence depolarizes. The fluorescence depolarization kinetics provide information about the rotational dynamics of the fluorophore. For simple, freely tumbling molecules, the depolarization kinetics can be characterized by a single time constant. In more complex molecules, such as derivatized peptides and proteins, the dynamics of fluorescence depolarization can be far more complex.[31]

We have performed time-resolved fluorescence anisotropy measurements with **1**−**4** to obtain some insight into the rotational freedom of the fluorescence donor in these peptides. In general, we find biphasic depolarization kinetics: a fast component with a time constant of ∼30 ps and slow component characterized by a ∼300-ps relaxation time. The amplitudes

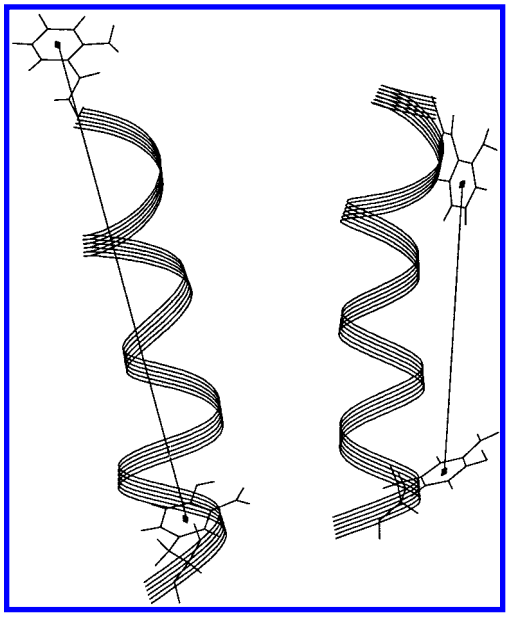

Figure 4. Two representative conformations from MD simulations of the relationship between donor−acceptor distance (r) and orientation in **3**.

of the two components are comparable. This observation contrasts with the single fast (<50 ps) component found in the depolarization dynamics of Abz−Gly. It is likely that the rapid depolarization component in the Abz-containing peptides corresponds to the rotation of the Abz side chain, while the slower component corresponds to tumbling dynamics of the entire peptide.

The fluorescence anisotropy data suggest that some systematic error in r_C values may be introduced by assuming that $\kappa = {}^2/_3$ (the value for random and uncorrelated orientation between donor and acceptor). MD calculations employing a fairly rigid peptide backbone indicate that the orientations of the phenyl groups in Abz and Tyr(NO_2) are not random and that there is possibly a correlation between distance and orientation (Figure 4). This is a general problem for donors and acceptors bound to rigid substrates. The problem of correlated distance and orientation can be ameliorated somewhat by using longer linkers to connect the chromophores to the backbone. This remedy, however, will be accompanied by the undesirable consequence of substantially broader donor−acceptor distance distributions.

Summary

Conformational interconversions play a key role in regulating biochemical transformations. The 31-Å Förster distance makes the 2-aminobenzamide/nitrotyrosine energy-transfer donor−acceptor pair well-suited for studying the conformations of proteins and medium-sized peptides. The donor−acceptor distances extracted from analyses of fluorescence decay kinetics in four modified peptides are in fair agreement with those predicted by molecular mechanics calculations. Fluorescence anisotropy measurements indicate that rapid side chain rotations only partially depolarize the Abz fluorescence in the four peptides that we have examined. Restricted rotation of the fluorescence probe is likely to be a common feature for many peptide-bound donors and acceptors.

Acknowledgment. This research was supported by a NATO Collaborative Research Grant (941068), the Carlsberg Foundation, and the Arnold and Mabel Beckman Foundation.

References and Notes

(1) Lewis, J. W.; Goldbeck, R. A.; Kliger, D. S.; Xie, X. L.; Dunn, R. C.; Simon, J. D. *J. Phys. Chem.* **1992**, *96*, 5243−5254.
(2) Dyson, H. J.; Wright, P. E. *Annu. Rev. Biophys. Biophys. Chem* **1991**, *20*, 519−538.
(3) Förster, T. *Ann. Phys. (Leipzig)* **1948**, *2*, 55−75.
(4) Wu, P.; Brand, L. *Anal. Biochem.* **1994**, *218*, 1−13.
(5) Beecham, J. M.; Haas, E. *Biophys. J.* **1989**, *55*, 1225−1236.
(6) Imperiali, B.; Rickert, K. W. *Proc. Natl. Acad. Sci. U.S.A.* **1995**, *92*, 97−101.
(7) Rischel, C.; Thyberg, P.; Rigler, R.; Poulsen, F. M. *J. Mol. Biol.* **1996**, *257*, 877−885.
(8) Meldal, M. The Solid-Phase Enzyme Inhibitor Library Assay. In *Combinatorial Peptide Library Protocols*; Cabilly, S., Ed.; Humana Press: Totowa, NJ, 1998; Vol. 87.
(9) Spetzler, J. C.; Westphal, V.; Winther, J. R.; Meldal, M. *J. Pept. Sci.* **1998**, *4*, 128−137.
(10) Mehta, S.; Meldal, M.; Ferro, V.; Duus, J. Ø.; Bock, K. *J. Chem. Soc., Perkin Trans. 1* **1997**, 1365−1374.
(11) Meldal, M.; Breddam, K. *Anal. Biochem.* **1991**, *195*, 141−147.
(12) Rischel, C.; Poulsen, F. M. *FEBS Lett.* **1995**, *374*, 105−109.
(13) Holm, A.; Meldal, M. Multiple Column Peptide Synthesis. In *Peptides 1988, Proceedings of the European Peptide Symposium*, 20th ed.; Jung, G., Bayer, E. W. d. G., Eds.; Berlin, 1989; pp 208−210.
(14) Meldal, M.; Holm, C. B.; Bojesen, G.; Jacobsen, M. H.; Holm, A. *Int. J. Pept. Protein Res.* **1993**, *41*, 250−260.
(15) Blankemeyer-Menge, B.; Nimtz, M.; Frank, R. *Tetrahedron Lett.* **1990**, *31*, 1701−1704.
(16) Rice, S. F.; Gray, H. B. *J. Am. Chem. Soc.* **1983**, *105*, 4571−4575.
(17) Demas, J. N.; Crosby, G. A. *J. Phys. Chem.* **1971**, *75*, 991−1024.
(18) Melhuish, W. H. *J. Phys. Chem.* **1961**, *65*, 229−235.
(19) Thormählen, I.; Straub, J.; Grigull, U. *J. Phys. Chem. Ref. Data* **1985**, *14*, 933−945.
(20) O'Connor, D. V.; Phillips, D. *Time-Correlated Single Photon Counting*; Academic Press: Orlando, FL, 1984.
(21) Večeř, J.; Kowalczyk, A. A.; Dale, R. E. *Rev. Sci. Instrum.* **1993**, *64*, 3413−3424.
(22) Dey, J. K.; Dogra, S. K. *Indian J. Chem.* **1990**, *29A*, 1153−1164.
(23) Dauber-Osguthorpe, P.; Roberts, V. A.; Osguthorpe, D. J.; Wolff, J.; Genest, M.; Hagler, A. T. *Proteins: Struct., Funct., Genet.* **1988**, *4*, 31−47.
(24) Lyu, P. C.; Marky, L. A.; Kallenbach, N. R. *J. Am. Chem. Soc.* **1989**, *111*, 2733−2734.
(25) Marqusee, S.; Baldwin, R. L. *Proc. Natl. Acad. Sci. U.S.A.* **1987**, *84*, 8898−8902.
(26) Mouritsen, S.; Meldal, M.; Rubin, B.; Holm, A.; Werdelin, O. *Scand. J. Immunol.* **1989**, *30*, 723−730.
(27) Ösapay, G.; Taylor, J. W. *J. Am. Chem. Soc.* **1992**, *114*, 6966−6973.
(28) Hirata, I. Y.; Cezari, M. H. S.; Nakaie, C. R.; Boschcov, P.; Ito, A. S.; Juliano, M. A.; Juliano, L. *Lett. Pept. Sci.* **1995**, *1*, 299−308.
(29) Williams, S.; Causgrove, T. P.; Gilmanshin, R.; Fang, K. S.; Callender, R. H.; Woodruff, W. H.; Dyer, R. B. *Biochemistry* **1996**, *35*, 691−697.
(30) Chou, P. Y.; Fasman, G. D. *Biochemistry* **1974**, *13*, 211−222.
(31) Lipari, G.; Szabo, A. *Biophys. J.* **1980**, *30*, 489−506.